

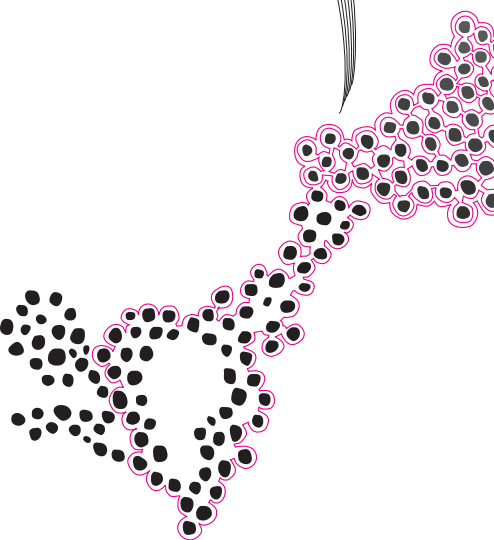
BSc Thesis Applied Mathematics
and Applied Physics

An analysis of Andreev bound states in a systems of topological insulators

William Schaarman

Supervisors:
Alexander Brinkman
Bernard Geurts

29th June 2020



Department of Applied Mathematics
Faculty of Electrical Engineering,
Mathematics and Computer Science

Department of Applied Physics
Faculty of Science and Technology

0.1 preface

This report was written as a Bachelor Assignment for the ICE group at the University of Twente. I would like to thank my supervisors Alexander Brinkman and Bernard Geurts for helping me with the different obstacles I encountered and for making me familiar with the subject matter. This assignment was in my opinion a very enjoyable one with a lot of difficulties but also with really beautiful results.

Abstract

In this thesis an overview is given of the current methods for theoretically deriving the conductance of a system constructed using topological insulators which can both be magnetic or superconducting. A special system is analysed from which the conductance is determined and put in context with the different variables used. The system itself has Andreev bound states involved which greatly increase the conductance at certain Energy levels. In the system the phase added by the traveling wave is also taken into account and analysed to see if this corresponds to the theory presented.

Keywords: Topological insulator, Superconductivity, Andreev bound states

Contents

0.1 preface	2
1 Introduction	1
2 Theory	1
2.1 The theory of superconductivity	2
2.2 Topological Insulators	4
2.3 Representation of the states	6
2.4 The system	6
2.4.1 Normal TI	7
2.4.2 Magnetic TI	8
2.4.3 Superconducting TI	9
2.5 Andreev bound states	9
2.6 Resonance in materials	10
3 Method	11
3.1 Numerical variables	11
3.2 Andreev bound states	11
3.3 General system	12
3.3.1 Definition of the angles	12
3.3.2 Example construction of TI/STI interface	13
3.3.3 Example construction of MTI/TI interface	13
3.3.4 Total system	14
3.3.5 Conservation of momentum	14
3.3.6 Conductance	15

4	Results	16
4.1	1D phase calculations	16
4.2	1D total system	16
4.3	2D phase calculations	17
4.4	2D system calculation	20
4.5	System conductance	24
5	Discussion	27
5.1	Limitations of the model	27
5.2	Expansion of the model	27
6	Conclusion	27
7	Future experiments	28

An analysis of Andreev bound states in a system of topological insulators

William Schaarman *

29th June 2020

1 Introduction

In the last two decades a lot of advancements have been made in physics regarding material science. One of the materials especially heavily studied is the topological insulator (TI).[1] One of the main properties of this material is that it can only conduct charged particles at the surface instead of in the bulk of the material. One of the major theoretical implications this has is that Majorana bound states can potentially occur in these materials.[2] In systems like these the spin-orbit coupling, which is also responsible for effects like the Zeeman effect, is a necessary ingredient for the Majorana fermions. These Majorana fermions can then be used to lead to future scientific progress towards the quantum computer where they can be applied to the qubits.

These Majorana bound states have already been demonstrated to exist in the past. A paper by the university of Delft demonstrated this by finding a zero-bias conductance peak.[3] This experiment was however preformed with a nanowire instead of topological insulators this thesis will look at.

One of the major discoveries that may lead to finding these Majorana fermions is Andreev reflection. The discovery of this effect together with the properties of topological insulators brings systems to mind which realize this fermion. One of the more recent additions is a paper on a system consisting of magnetic and superconducting topological insulators (called MTI and STI respectively).[4]

The main contribution of this paper is to expand on a previously analysed system consisting of an MTI and STI. More specifically a normal TI will be added between the MTI and STI which gives a more general system when compared to previously analysed systems. This extra TI gives rise to two new variables which can be tuned. One of these is the chemical potential of the TI and the other is the length of the TI. The calculations of this system will be presented with the necessary theory which is required to get a deeper insight into the subject. Also a set of constraints is given for which the system is valid.

2 Theory

In the theory a certain baseline will be established which is necessary to understand the results of the thesis. Firstly, in section 2.1 the BCS theory will be discussed which describes superconductivity in materials. Then, in section 2.2, Topological insulators will be

*Email: w.a.schaarman@student.utwente.nl

discussed and the properties of these materials which will be used in the thesis. Afterwards, in section 2.3 and 2.4 the basic spinors of the system will be given using the Dirac notation of the hamiltonians. The next theory that is discussed are Andreev bound states and their properties, which will also be referred to as ABS. These can be found in section 2.5. The last topic in the theory is a quick look at the phase materials can add to the wavefunction, which can be found in section 2.6.

2.1 The theory of superconductivity

It was discovered that at low temperatures certain composites and metals get special properties. One of these properties is the phenomenon called superconductivity. Superconductivity is the phenomenon where the resistance in a material decreases significantly as function of the temperature near the critical temperature.

The first paper to model this phenomena clearly was the BCS paper.[5] This theory, developed by Bardeen, Cooper and Schrieffer, relies on electrons forming pairs called Cooper pairs. Essentially, these pairs would then behave not as a two separate fermions but like a boson. This change of behaviour allows the pairs to go into a lower energy state which reduces the resistance of the material to zero, thus creating superconductivity.

To go into more detail, we consider an electron in state \mathbf{k} in a metal at $T = 0$, which is the absolute zero. This electron can go into another state \mathbf{k}' by creating a phonon \mathbf{q} . This gives us the equation $\mathbf{k} = \mathbf{k}' + \mathbf{q}$. This phonon can then be absorbed by another electron. We can describe the total interaction by $\mathbf{k}_1 + \mathbf{k}_2 = \mathbf{k}'_1 + \mathbf{k}'_2$. In figure 1 you can see this interaction displayed in a Feynman diagram.

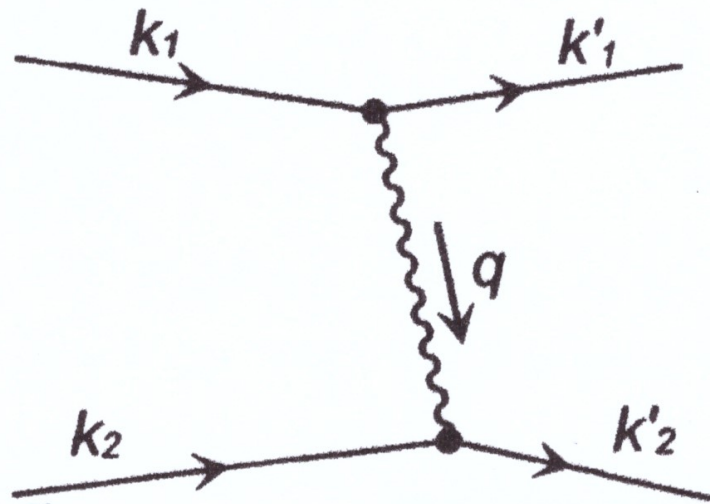


FIGURE 1: Feynman diagram of the interacting electron pair. This interaction is able to occur through the exchange of a phonon.[6]

Since an electron moves from one state to another, an oscillation in the electron density is created at the frequency $\omega = (\epsilon_{k_1} - \epsilon_{k_1'})/\hbar$. These oscillations can create a negatively charged area. Since the ions in the lattice are positively charged they will move towards

this area. This area now becomes positively charged due to the presence of the ions. This can be clearly seen in figure 2. Since the ions are too massive to travel back in a short time, this now positive charged area attracts a second electron which together with the first electron creates a Cooper pair.

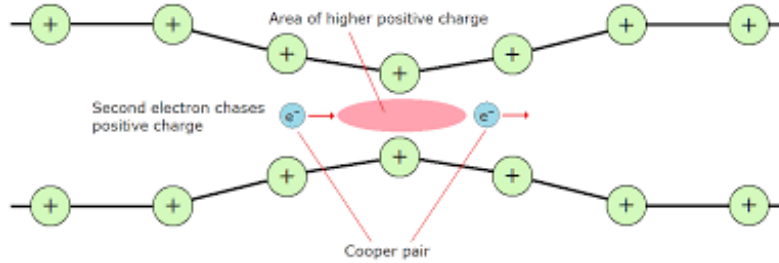


FIGURE 2: Schematic overview of a cooper pair interacting. It can clearly be seen that an after an electron passes through an area between positive ions, the ions will create a positively charged area which in turn attracts a second electron. The two electrons are called a cooper pair. [7]

Only if this vibration is smaller than the Debye frequency, so $\omega < \omega_D$, atoms will be attracted to the, previously mentioned, positive area. The Debye frequency is the characteristic frequency of the system. This gives us the identity that the electrons can only interact if $|\epsilon_k - \epsilon_f| \leq \hbar\omega_D$.

Now we can analyse the case $\mathbf{k}_1 + \mathbf{k}_2 = \mathbf{k}'_1 + \mathbf{k}'_2$ more clearly. Because of conservation of momentum electrons which start at \mathbf{k} can only scatter to a set amount of states for a given \mathbf{q} . This can be schematically give by figure 3 below.

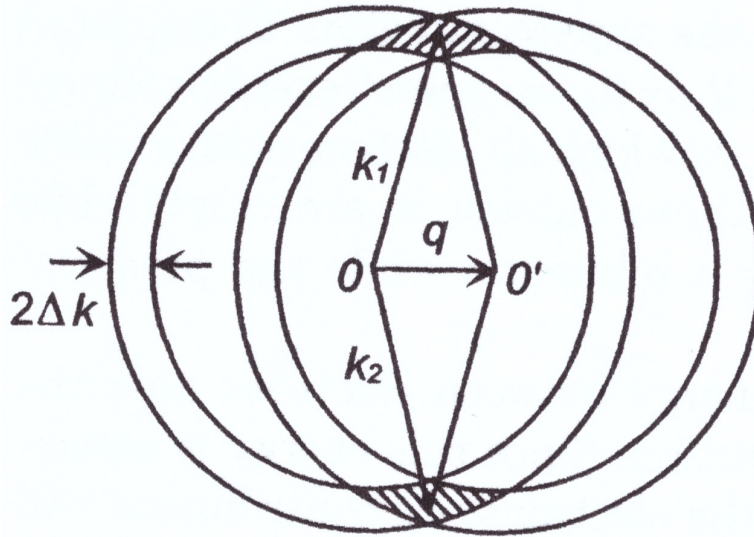


FIGURE 3: Schematic overview of the number of states an electron pair can scatter to (Dark area). \mathbf{k}_1 and \mathbf{k}_2 represent the initial state of the electrons and \mathbf{q} represents the phonon which is exchanged between the two. $2\Delta\mathbf{k}$ is the area in which is close enough to the Fermi level such that scattering can occur.[6]

Now we are ready to look at a new function of \mathbf{k} , which is $v_{\mathbf{k}}^2$. This function gives the probability that the state $(\mathbf{k}, -\mathbf{k})$ is occupied. Using this function we can also define $u_{\mathbf{k}}^2 = 1 - v_{\mathbf{k}}^2$ which gives the probability that the state $(\mathbf{k}', -\mathbf{k}')$ is occupied. These constants can later be found back in the hamiltonian and spinors of the system.

One of the aspects of a superconductor that was explained by the BCS theory is the superconducting gap. This gap in the band structure of a superconductor is a certain set of states which cannot be occupied around the Fermi level. This has as result that particles will not be able to enter this state and thus reflect in some way of the material.

2.2 Topological Insulators

As said in the introduction of this thesis topological insulators are materials which have the property of only allowing conduction on the surface of the material and not inside the material. This gives the material interesting properties with regards to the states of the particles in this material. One of the consequences is that the dispersion curves of these materials are linear instead of quadratic, which is usually the case normal conductors.[1]

Among the topological insulators (in short TIs) there are different kinds. One distinction which can easily be made are the 2D and 3D topological insulators. A 3D topological insulator is insulated in the bulk of the material but is able to conduct particles at the surface. A 2D topological insulator insulates the states on the surface and will only be able to conduct particles on the edges of the material. This gives rise a 2D and 1D system respectively for the conducting states.

Another distinction can be made when looking at TIs with extra properties. Two of these

are the magnetic TI[8] (MTI) and the superconducting TI (STI). The MTI has a built in magnetic field which can interact with the electrons and holes in the material. The STI has all the properties of a superconducting material with the addition that the material is only able to conduct electrons and holes on the surface.

The linear dispersion relation in a TI is also named a Dirac cone. These cones describe a linear relation between the \mathbf{k} and the energy E of the particles. The dirac cones cross each other at a certain point. The value at this point is given by the chemical potential μ and this point is called the Dirac point. In MTIs and STIs these Dirac cones are not linear any more. An overview of the dispersion relation of all three materials with their respective constants can be seen in figure 4 below.

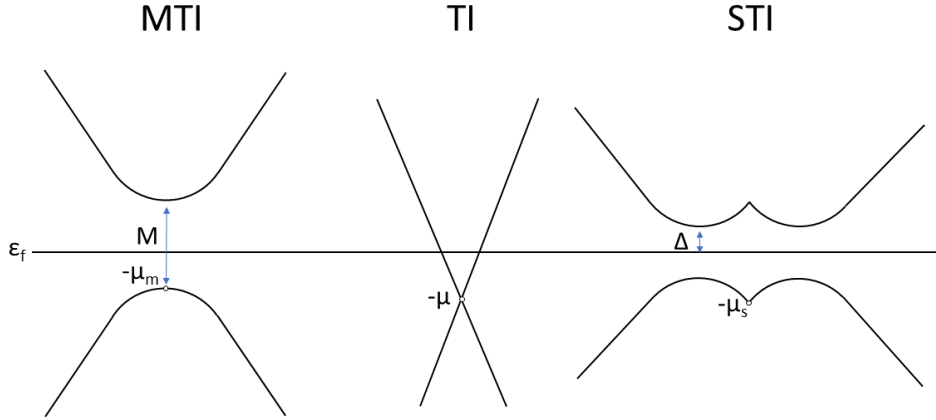


FIGURE 4: Here the dispersion relation is given for the different topological insulators. Also the definition of the different constants used in the paper are given. This system already represents the system that will be analysed except that it misses an TI on the left side of the MTI.

The dispersion relations are described by specific formulas which can easily be found when solving the hamiltonian. The Hamiltonians which should be solved to give these equations is found in section 2.4. To give an overview of the dispersion relations you can look in equation 1, 2 and 3 .

$$\text{TI: } E = \hbar v_f |\mathbf{k}| - \mu \quad (1)$$

$$\text{MTI: } E = \sqrt{(\hbar v_f |\mathbf{k}|)^2 + M^2} - \mu_m \quad (2)$$

$$\text{STI: } E = \sqrt{\Delta^2 + (\hbar v_f |\mathbf{k}| - \mu_s)^2} \quad (3)$$

In the latter two cases we can see that if $|\mathbf{k}|$ is sufficiently large in comparison to the other variables then they reduce to the the normal TI case which is linear. Also in these cases it is considered that $\mu, \mu_S, \mu_m > E$ for simplicity. This gives us the case where our particles will always be far above the Dirac point. The calculations of the dispersion relations are done in the sections going more in depth in the system.

2.3 Representation of the states

In this paper the Dirac notation will be used for wave functions. This implies that the wave function will be described by spinors. These spinors consist wave functions which each move in a direction. From these spinors a basis can be established which describes the whole system. For this thesis the basis 4 will be used.

$$\Psi = \begin{pmatrix} \psi_{\uparrow} \\ \psi_{\downarrow} \\ \psi_{\uparrow}^* \\ \psi_{\downarrow}^* \end{pmatrix} \quad (4)$$

To give a bit more clarification on the basis. The two upper parts resemble an electron with a spin up and down component while the lower two parts are a hole with a spin up and down component. For the TI and MTI case we have the electrons and holes have separate wave functions which are not connected with each other while in the STI case they are connected.

2.4 The system

In this paper we will look at the properties of a system composed of three different Topological insulators, the MTI, TI and STI. Since topological insulators can only conduct a current on the surface it is sufficient to analyse this system in 2D. A schematic overview of the exact system with described distances is given in figure 5

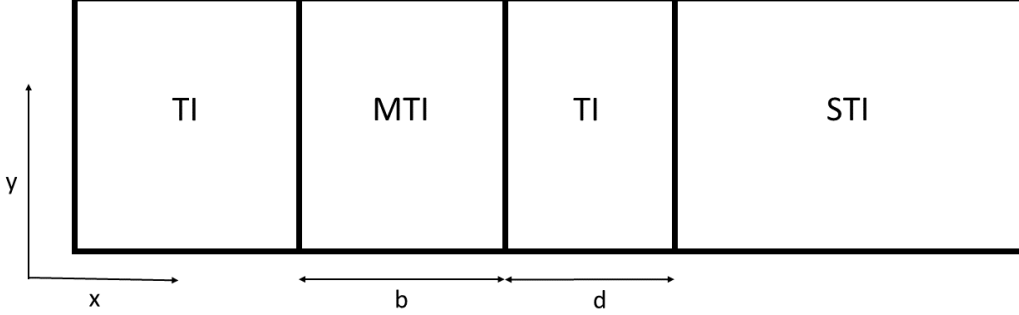


FIGURE 5: A total overview of the system where b and d describe the width of the MTI and TI respectively. The origin of the system will be chosen at the TI/STI interface. The system extends to infinity in all directions.

In this system it is important to notice that the barriers are parallel to the x-axis. This implies that any spinor in the x-direction must be evanescent while it is always wavelike in the y-direction. This implies that a test function of the form

$$\psi(x, y) = \begin{pmatrix} a \\ b \\ c \\ d \end{pmatrix} e^{i\hat{k}x} e^{ik_y y} \quad (5)$$

would be sufficient in describing all wave functions as long as \hat{k} is considered purely real for a conducting phase and \hat{k} is purely imaginary in a barrier.

In the whole system only a few specific cases will be considered which should be the most interesting. To get Andreev bound states, it is necessary that the MTI serves as a barrier. This implies that $M > \mu_m$. Apart from that only calculations above the Dirac cone will be taken into account. This in turn implies $\mu > E$ for the MTI, STI and TI. Also we want to consider the case that $\Delta > |E|$. This implies that the superconducting gap is larger than the energies considered implying that we have no conducting spinor in the STI without an evanescent part. This specific configuration is chosen to focus on the Andreev bound states.

2.4.1 Normal TI

By using the Dirac notation we can write the Hamiltonian for the electrons in a TI like given in formula 6.[9]

$$\hat{H}_{TI}(\mathbf{k}) = v_f \left(\hat{\sigma}_x \frac{\hbar}{i} \frac{\partial}{\partial x} + \hat{\sigma}_y \frac{\hbar}{i} \frac{\partial}{\partial y} \right) - \mu \mathbb{1} \quad (6)$$

In this equation σ_x and σ_y are the Pauli matrices of the form

$$\sigma_x = \begin{pmatrix} 0 & 1 \\ 1 & 0 \end{pmatrix}$$

and

$$\sigma_y = \begin{pmatrix} 0 & -i \\ i & 0 \end{pmatrix}$$

The solution to this hamiltonian is needed for 4 cases in total. We need a solution for electrons traveling in the positive and negative x direction. We also need a solution for holes traveling in the positive and negative x direction. The hamiltonian above is however only given for electrons. For holes we need to use the hamiltonian $-\hat{H}_{TI}^*(-\mathbf{k})$ to describe the specific properties of the holes. We can thus describe the total system as

$$H = \begin{pmatrix} \hat{H}(\mathbf{k}) & 0 \\ 0 & -\hat{H}^*(-\mathbf{k}) \end{pmatrix}$$

As can be seen we can divide this system into two separate parts each described by one hamiltonian. One system describes the electrons while the other describes the holes. The eigenvectors of each of these systems will describe the solutions to the system.

Using the identity $\hat{H}\psi = E\psi$, we can solve this system by using a test function $\psi(x, y) = \begin{pmatrix} \Phi \\ \chi \end{pmatrix} e^{ik_x x} e^{ik_y y}$. We take this test function as a simplification of the aforementioned function 5.

For electrons traveling in the positive direction we get the solution. $\psi(x, y) = \frac{1}{\sqrt{2}} \begin{pmatrix} 1 \\ e^{i\theta} \end{pmatrix} e^{ik_x x} e^{ik_y y}$. For electrons traveling in the negative x direction we get $\psi(x, y) = \frac{1}{\sqrt{2}} \begin{pmatrix} 1 \\ -e^{-i\theta} \end{pmatrix} e^{-ik_x x} e^{ik_y y}$. This does require an additional identity to be established which is $\hbar v_f |k| - \mu = E$ which is quickly recognised as the dispersion relation of a TI. We also have $\theta = \tan(k_y/k_x)$ and $|k| = \sqrt{k_x^2 + k_y^2}$.

For holes we can do exactly the same method and we will arrive at the same solutions with one difference, the identity is $\hbar v_f |k| + \mu = E$.

2.4.2 Magnetic TI

For the MTI a similar approach can be taken as for the TI. The hamiltonian for the MTI is given by

$$\hat{H}_{MTI} = v_f \left(\hat{\sigma}_x \frac{\hbar}{i} \frac{\partial}{\partial x} + \hat{\sigma}_y \frac{\hbar}{i} \frac{\partial}{\partial y} \right) + M \hat{\sigma}_z - \mu_m \mathbb{1} \quad (7)$$

Here σ_z is a Pauli matrix described by

$$\sigma_z = \begin{pmatrix} 1 & 0 \\ 0 & -1 \end{pmatrix}$$

In this thesis only the case where $M > \mu_m$ is taken into account. The implications of this is that the MTI will serve as a barrier where only evanescent waves can be present, i.e. there are no traveling waves in the x direction in the MTI. This means it is more

advantageous to start with a different test function compared to the TI. The test function which is used is $\psi(x, y) = \begin{pmatrix} \Phi \\ \chi \end{pmatrix} e^{\kappa x} e^{ik_y y}$, we get the normalised solutions $\psi(x, y) = \frac{1}{\sqrt{A_+}} \begin{pmatrix} E + \mu_m + M \\ i\hbar v_f \kappa_e + i\hbar v_f k_y \end{pmatrix} e^{-\kappa_e x} e^{ik_y y}$ and $\psi(x, y) \frac{1}{\sqrt{A_-}} = \begin{pmatrix} E + \mu_m + M \\ -i\hbar v_f \kappa_e + i\hbar v_f k_y \end{pmatrix} e^{\kappa_e x} e^{ik_y y}$, with $A_{\pm} = (E + \mu_m + M)^2 + (\hbar v_f \kappa_e \pm \hbar v_f k_y)^2$. You can also derive the identity $(E + \mu_m)^2 = M^2 + (\hbar v_f k_y)^2 - (\hbar v_f \kappa_e)^2$ which gives the dispersion relation in the MTI.

The wave function for the holes in this material are calculated in a similar manner in comparison to the TI. Again, if we take as hamiltonian $-\hat{H}^*(-\mathbf{k})$ and the same test function as previously we find $\psi(x, y) = \frac{1}{\sqrt{B_-}} \begin{pmatrix} E - \mu_m - M \\ i\hbar v_f \kappa_h - i\hbar v_f k_y \end{pmatrix} e^{-\kappa_h x} e^{ik_y y}$ and $\psi(x, y) \frac{1}{\sqrt{B_+}} = \begin{pmatrix} E - \mu_m - M \\ -i\hbar v_f \kappa_h - i\hbar v_f k_y \end{pmatrix} e^{\kappa_h x} e^{ik_y y}$ with the identity $(E - \mu_m)^2 = M^2 + (\hbar v_f k_y)^2 - (\hbar v_f \kappa_h)^2$ and $B_{\pm} = (E - \mu_m - M)^2 + (\hbar v_f \kappa_h \pm \hbar v_f k_y)^2$.

2.4.3 Superconducting TI

The STI will be evaluated such that $|E| < \Delta$. This implies that particles will be used which have an energy lower than the superconducting band gap. In this range no conducting state is possible so we get a special case where the wave function is a combination of a traveling wave and an evanescent wave.

The hamiltonian for the STI is given by[10]

$$\hat{H}_{STI} = \begin{pmatrix} \hat{H}_{TI}(\mathbf{k}) & \hat{\Delta} \\ -\hat{\Delta} & -\hat{H}_{TI}^*(-\mathbf{k}) \end{pmatrix}$$

Where $\hat{\Delta} = i\Delta\sigma_y$

In contrast to the previous two hamiltonians, there is a clear connection between electrons and holes in this hamiltonian.

This will result in two relevant solutions which are $\psi(x, y) = \begin{pmatrix} a \\ b \\ c \\ d \end{pmatrix} e^{i\hat{k}x} e^{ik_y y}$ where $\hat{k} = k_x + i\kappa$ with $k_x > 0$. We have $k_x > 0$ since the waves can only travel in the positive x-direction. Using this test function and the given restriction we get the two solutions $\psi_e(x, y) = \frac{1}{2} \begin{pmatrix} e^{i\theta_S} \\ -\frac{\chi_e^2}{\Delta} e^{i\theta_S} \\ \frac{\chi_e^2}{\Delta} \end{pmatrix} e^{i\hat{k}_e x} e^{ik_y y}$ and $\psi_h(x, y) = \frac{1}{2} \begin{pmatrix} e^{i\theta_S} \\ -\frac{\chi_h^2}{\Delta} e^{i\theta_S} \\ \frac{\chi_h^2}{\Delta} \end{pmatrix} e^{i\hat{k}_h x} e^{ik_y y}$.

In the above spinors we have defined $\chi_i = \sqrt{E + \mu_s - \hbar v_f |k_i|}$ with $k_e = \mu + \sqrt{E^2 - \Delta^2}$ and $k_h = \mu - \sqrt{E^2 - \Delta^2}$. We also define $\theta_S = \arctan\left(\frac{k_y}{k_x}\right)$

This also results in the identity $(\hbar v_f |\hat{k}| - \mu_S)^2 + \Delta^2 = E^2$ which can be rewritten as $\mathbf{k} = \frac{\pm\mu \pm i\sqrt{\Delta^2 - E^2}}{\hbar v_f}$. If we compare that to a previous expression $\hat{k} = k_x + i\kappa$ and consider that we do not necessarily need to take $|\hat{k}|$ real but as an imaginary number. Then we find that $k_x = \pm\mu_S/\hbar v_f$ and $\kappa = \pm\sqrt{\Delta^2 - E^2}/\hbar v_f$.

2.5 Andreev bound states

Andreev reflection is a phenomenon occurring at an interface between a superconductor and a conductor. If you would consider a wave function describing an electron traveling towards the interface from the TI, then instead of scattering back into an electron in the

opposite direction it can scatter back as a hole. If we consider this situation with particles, we can view it as one electron entering the STI and pairing up with an electron in the STI. However because of conservation of charge this implies that a hole is created which travels in the opposite direction.

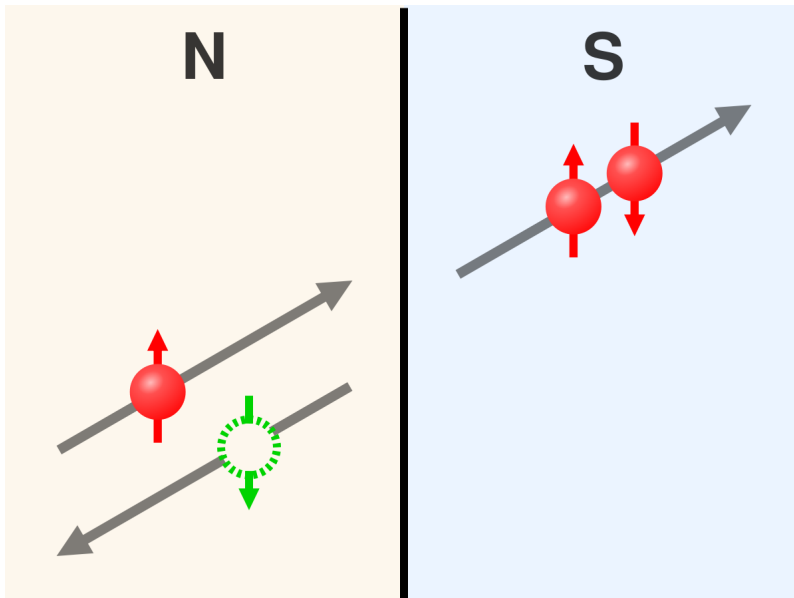


FIGURE 6: Andreev reflection with a normal metal (N) and a superconductor (S) [11]

When consider a larger system, say an STI/TI/STI system with Andreev reflection on both interfaces. We can imagine a particle interacting with one interface and returning a hole in the opposite direction. On the other interface this hole can interact such that a hole pair is created in the superconductor which returns an electron again. This loop is called an Andreev bound state.

In the system that is analysed an Andreev bound state can also be observed. However instead of the second STI/TI interface the one STI/TI interface is considered twice in one loop since the MTI will serve as a barrier from which electrons and holes can reflect.

For an Andreev bound state to be able to exist it is important that the phase received by the wave function in the bound state is of the magnitude $2\pi n$ with n any integer. The phase a wave function receives is defined as $\tan(\alpha) = \frac{Im(r)}{Re(r)}$ where r is the reflection constant and α is the phase. This is only correct if $Re(r) > 0$ otherwise an extra phase of π must be added.

2.6 Resonance in materials

As was just explained in the system the ABS will be especially interesting. However, the interfaces are not the only way for a wavefunction to gain a phase. A phase can also be gained by a wave by traveling through the material. These phases can be clearly seen by looking at the different spinors. If you consider the exponent after each of the spinors then you can conclude that for a exponent which is not close to 0, the wavefunction gains a measurable phase.

The added phase is easily calculated as $\alpha_d = \arg(e^{ik_x x})$. In our system the distance is d however since the wavefunction of an ABS reflects 4 times of a surface and thus travels 4 times the distance. This implies that a length of $4d$ needs to be considered instead.

Using the above phase formula we can determine for what distances d we should have a phase which does not contribute to the overall phase. This is however only useful for the 1D case as in 2D case the distance is not just determined by the thickness of the TI but also by the angle the particle travels with in comparison to the interface. In 1D we have $2\pi n = 4dk_x$. With the approximation that for $E \ll \mu$ we have that $\frac{d\mu}{\hbar v_f} = \frac{n\pi}{2}$.

Another resonances which is possible in this system is an electron or hole reflecting between the MTI/TI interface and TI/STI interface without Andreev reflection. For this reflection to be dominant it is necessary that Andreev reflection occurs less than the normal reflection. A similar equation can be established for this case. Since this resonance only requires two reflections the distance is $2d$ instead of $4d$. This implies that we get $\frac{d\mu}{\hbar v_f} = n\pi$.

3 Method

To actually analyse the system two variants will be taken into account, one 1D and one 2D. First of the limits of the system will need to be analysed which is done in 3.1. These systems can be divided into two parts. For each, the calculations of the Andreev bound states will be done using the phase of the different reflection constants, an explanation of this is given in section 3.2. The other approach which is taken is that the whole system will be analysed at once. This implies a system of equations that needs to be solved which is given in section 3.3.4. For both methods the programs Matlab and Mathematica will be used. The first one is mainly used for numeric calculations while the latter is used to easily find analytic expressions. In the sections 3.3.3 and 3.3.2 an overview is given on how the scattering equations are set up using the proper definitions.

3.1 Numerical variables

To make the numerical program easier to work with and use it was chosen that $\hbar = 1$ and $v_f = 1$, which are Planck's constant and the Fermi velocity respectively. As said before we will also only look at the case where $\mu_m, \mu_S, \mu \geq \Delta > |E|$, $M > \mu_m > 0$, $\mu > 0$ and $\mu_S > 0$. This is done such that the MTI serves as a barrier. Also the STI does not conduct the electrons without some evanescent wave being present. Also, to simplify the system the chemical potential of the two TIs is taken equal.

Another subtle change is that all variables except d , b , θ and θ_S will be made dimensionless by dividing them by Δ . In the text these variables will be referred to with a tilde above their respective symbol. An example is $\tilde{E} = E/\Delta$.

3.2 Andreev bound states

As was said in more detail in the section Andreev bound states in the theory, for an Andreev bound state to exist the condition must hold that the phase of a loop is $2\pi n$ with n an integer. In the whole system there is one such loop where an Andreev bound state could arise. This bound state arises in between the MTI/TI interface and the TI/STI interface. The whole bound state is described by the following loop: An electron can have Andreev reflection on the TI/STI surface. Then the resulting hole reflects of the MTI/TI interface. After this Andreev reflection can take place again at the TI/STI interface after which the

electron can reflect at the MTI/TI interface again. This whole loop can be described by 4 reflection constants which are respectively, r_{eh} , r_{hh} , r_{he} and r_{ee} .

As was described before it is necessary for the calculations of the phase of the wave function that these reflection constants are known. Each of these constants can be calculated by considering just the one interface at $x=0$ as the place of the interface does not influence the phase of the wave function. Then for each of the reflection constants we can calculate the phase and add them together and see for what conditions they are a multiple of 2π . This gives us the formula

$$2\pi n = \alpha_{ee} + \alpha_{eh} + \alpha_{he} + \alpha_{hh} \quad (8)$$

where α_{ij} describes a particle i before the reflection and j after the reflection. Notice that in this case the phase gained by the wave function traveling through the TI is not taken into account.

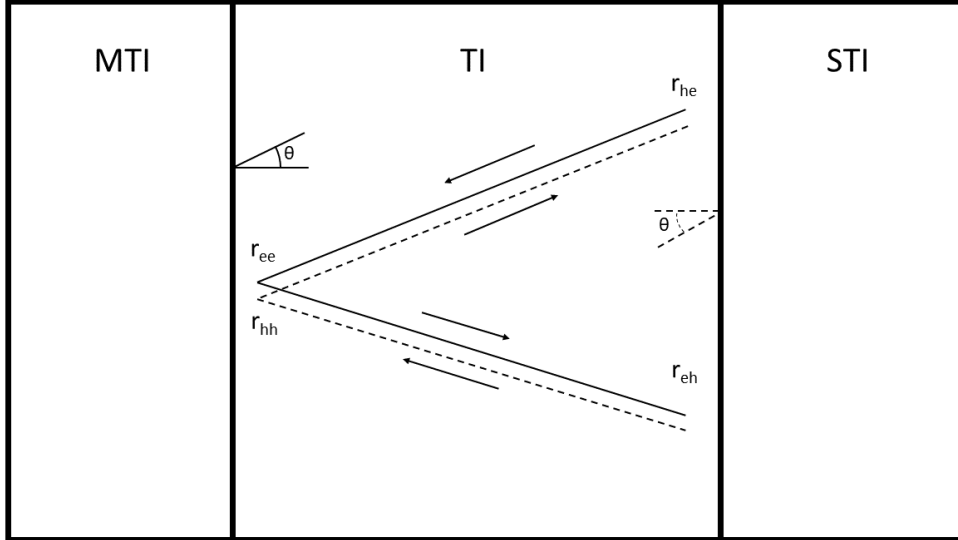


FIGURE 7: A schematic overview of the Andreev bound state in the system. The solid black line describes the electron moving while the dashed line describes the holes and their direction. In the figure the definition of θ is also given for both the electrons and holes.

3.3 General system

3.3.1 Definition of the angles

In figure 7 the definition of the angles used can be found. In this definition of θ the result for the holes and electrons is different. This is the result of the reversed \mathbf{k} vector described in the hamiltonian of the holes. This implies that an electron traveling in the negative x-direction is described by $\psi_e(\pi - \theta)$ while a hole traveling in the negative x-direction is described by $\psi_h(\theta)$. In the positive direction these would be $\psi_e(\theta)$ and $\psi_h(\pi - \theta)$ respectively. Since there is no traveling wave in the MTI no angle will be considered here however in the STI an angles does need to be defined. In the STI we get for the electron-like particle $\psi(\theta_S)$ while for the hole-like particle we get $\psi(\pi - \theta)$.

3.3.2 Example construction of TI/STI interface

To do the calculations of the system it is necessary to construct the scattering equations at each interface. Here a quick overview will be given on how to construct these equations for the TI/STI interface for an incoming electron.

First we start of by considering the particles which interact with the interface. Since there is an incoming electron we can expect a reflected electron or a reflected hole in the TI. In the STI both a hole-like and electron-like state will need to be considered. Considering the wave of incoming electron has a amplitude of 1 and that the wave functions must be continuous at the interface we get the following equality.

$$\psi_e(\theta) + r_{eh}\psi_h(\theta) + r_{ee}\psi_e(\pi - \theta) = t_{ee}\psi_e(\theta) + t_{eh}\psi_h(\pi - \theta) \quad (9)$$

In this equation to the left of the equality sign spinors in the TI are considered while on the right of the equality sign spinors in the STI are considered. Using the spinors established in section 2.4 we can construct the total scattering equation.

$$\frac{1}{\sqrt{2}} \begin{pmatrix} 1 \\ e^{i\theta} \\ 0 \\ 0 \end{pmatrix} + \frac{r_{ee}}{\sqrt{2}} \begin{pmatrix} 1 \\ -e^{-i\theta} \\ 0 \\ 0 \end{pmatrix} + \frac{r_{eh}}{\sqrt{2}} \begin{pmatrix} 0 \\ 0 \\ 1 \\ -e^{-i\theta} \end{pmatrix} = \frac{t_{ee}}{2} \begin{pmatrix} 1 \\ e^{i\theta} S \\ -\frac{\chi_e^2}{\Delta} e^{i\theta} S \\ \frac{\chi_e^2}{\Delta} \end{pmatrix} + \frac{t_{eh}}{2} \begin{pmatrix} -e^{-i\theta} S \\ \frac{\chi_h^2}{\Delta} e^{-i\theta} S \\ \frac{\chi_h^2}{\Delta} \end{pmatrix} \quad (10)$$

In the above equation the interface is considered to be at $x=0$. Since there are 4 equations with 4 unknowns this system can be solved for r_{eh} which gives the coefficient of the Andreev reflection. Afterwards the argument of this reflection constant can be taken to determine the phase that is added by the reflection.

3.3.3 Example construction of MTI/TI interface

On the MTI/TI interface the approach is the same as with the TI/STI interface however this interface is considerably easier. First off, if we consider an incoming electron then either the electron reflects back or it tunnels through the MTI. This implies that we only need to consider two extra spinors and thus solve a system with two unknowns instead of four. As before, we can describe the spinors at the interface in terms of the angles. This gives us the following equation.

$$\psi_e(\pi - \theta) + r\psi_e(\theta) = t\psi_{MTI,e} \quad (11)$$

Here we consider the amplitude of the wavefunction for the incoming electron to be one. Using this equation and considering that the interface lies at $x=0$, we can describe the entire interface with the spinors from section 2.4 to give us

$$\frac{1}{\sqrt{2}} \begin{pmatrix} 1 \\ -e^{-i\theta} \end{pmatrix} + \frac{r}{\sqrt{2}} \begin{pmatrix} 1 \\ e^{i\theta} \end{pmatrix} = \frac{1}{\sqrt{A_-}} \begin{pmatrix} E-M-\mu_m \\ -i\kappa_e + ik_y \end{pmatrix} \quad (12)$$

3.3.4 Total system

The whole 2D system can however not be described by just the Andreev bound state. To actually get results on the conductivity of the system it is necessary to take the whole system into account.

To do the calculations for the total system each interface of two materials needs to be taken into account. At every point in the system the wave function must be continuous. This gives a set of 12 scattering equations with 12 unknown variables which are the amplitudes of the different parts of the wave function. Since the exponent of the STI is the most complicated the TI/STI interface is chosen as the origin as to eliminate it. The total system is given below.

$$\left\{ \begin{array}{l}
 \frac{e^{-i(b+d)k_e}}{\sqrt{2}} + C_1 \frac{e^{i(b+d)k_e}}{\sqrt{2}} = C_2 \frac{e^{-(b+d)\kappa_e(E+M+\mu_m)}}{\sqrt{A_-}} + C_3 \frac{e^{(b+d)\kappa_e(E+M+\mu_m)}}{\sqrt{A_+}} \\
 \frac{e^{-i(b+d)k_e+i\theta}}{\sqrt{2}} - C_1 \frac{e^{i(b+d)k_e-i\theta}}{\sqrt{2}} = C_2 \frac{e^{-(b+d)\kappa_e(-i\kappa_e+ik_{ye})}}{\sqrt{A_-}} + C_3 \frac{e^{(b+d)\kappa_e(i\kappa_e+ik_{ye})}}{\sqrt{A_+}} \\
 C_2 \frac{e^{-d\kappa_e(E+M+\mu_m)}}{\sqrt{A_-}} + C_3 \frac{e^{d\kappa_e(E+M+\mu_m)}}{\sqrt{A_+}} = C_4 \frac{e^{-idk_e}}{\sqrt{2}} + C_5 \frac{e^{idk_e}}{\sqrt{2}} \\
 C_2 \frac{e^{-d\kappa_e(-i\kappa_e+ik_y)}}{\sqrt{A_-}} + C_3 \frac{e^{d\kappa_e(i\kappa_e+ik_y)}}{\sqrt{A_+}} = C_4 \frac{e^{-idk_e i\theta}}{\sqrt{2}} - C_5 \frac{e^{idk_e-i\theta}}{\sqrt{2}} \\
 C_4 \frac{1}{\sqrt{2}} + C_5 \frac{e^{-i\theta}}{\sqrt{2}} = C_8 \frac{1}{2} + C_9 \frac{1}{2} \\
 C_4 \frac{1}{\sqrt{2}} + C_5 \frac{e^{i\theta}}{\sqrt{2}} = C_8 \frac{e^{i\theta S}}{2} - C_9 \frac{e^{-i\theta S}}{2} \\
 C_6 \frac{1}{\sqrt{2}} + C_7 \frac{1}{\sqrt{2}} = C_8 \frac{e^{i\theta S}(E+i\sqrt{\Delta^2-E^2})}{2} - C_9 \frac{e^{-i\theta S}(E-i\sqrt{\Delta^2-E^2})}{2} \\
 C_6 \frac{e^{i\theta}}{\sqrt{2}} - C_7 \frac{e^{-i\theta}}{\sqrt{2}} = -C_8 \frac{(E+i\sqrt{\Delta^2-E^2})}{2} + C_9 \frac{e^{-i\theta S}(E-i\sqrt{\Delta^2-E^2})}{2} \\
 C_{10} \frac{e^{-d\kappa_h(E-M-\mu_m)}}{\sqrt{B_+}} + C_{11} \frac{e^{d\kappa_h(E-M-\mu_m)}}{\sqrt{B_-}} = C_6 \frac{e^{-idk_h}}{\sqrt{2}} + C_7 \frac{e^{idk_h}}{\sqrt{2}} \\
 C_{10} \frac{e^{-d\kappa_h(i\kappa_h-ik_y)}}{\sqrt{B_+}} + C_{11} \frac{e^{d\kappa_h(-i\kappa_h-ik_y)}}{\sqrt{B_-}} = C_6 \frac{e^{-idk_h+i\theta}}{\sqrt{2}} - C_7 \frac{e^{idk_h-i\theta}}{\sqrt{2}} \\
 C_{12} \frac{e^{i(b+d)k_h}}{\sqrt{2}} = C_{10} \frac{e^{(b+d)\kappa_h(E-M-\mu_m)}}{\sqrt{B_+}} + C_{11} \frac{e^{-(b+d)\kappa_h(E-M-\mu_m)}}{\sqrt{B_-}} \\
 -C_{12} \frac{e^{i(b+d)k_h-i\theta}}{\sqrt{2}} = C_{10} \frac{e^{(b+d)\kappa_h(-i\kappa_h-ik_{yh})}}{\sqrt{B_+}} + C_{11} \frac{e^{-(b+d)\kappa_h(i\kappa_h-ik_{yh})}}{\sqrt{B_-}}
 \end{array} \right. \quad (13)$$

This system is given in 2D but will also be calculated in 1D. To transform these equations to the 1D case it is necessary that $\theta = 0$ and $k_y = 0$. This gives a new set of equations which are easier to solve.

3.3.5 Conservation of momentum

When the expressions of the different constants are determined a lot of different variables will define them. To reduce the number of variables describing these equations the conservation of certain variables should be considered.

Firstly, k_y will always be conserved across the TI, MTI and STI. This is the consequence of particles not changing their velocity in the y-direction as the interface is parallel in this direction. This implies we can take the k_y defined by the TI for all k_y in the solution as this one is the easiest to define.

Another consequence of the conservation of momentum in the y-direction is that at the TI/STI interface an expression for θ_S can be defined as function of θ . This equation is

given in equation 14.

$$\sin(\theta)\mu = \mu_S \sin(\theta_S) \quad (14)$$

This implies the reflection constant can be defined by the variables μ_S , μ_m , μ , Δ , θ , E , d and b .

Applying equation 14 does imply that we must conclude that it is uncertain if the answer is correct for $\frac{\mu_S}{\mu} < 1$. By using a numerical example like $\theta = \pi/2$ and $\frac{\mu_S}{\mu} = \frac{1}{2}$ we can see that $\sin(\theta_S) = 2$ which is not possible for $\theta_S \in [-\pi/2, \pi/2]$. This issue is solved by not taking the reflection into consideration when this is the case.

3.3.6 Conductance

The variables C_1 and C_{12} are especially interesting as they can easily define the current. The constant $|C_1|^2$ gives us the probability of a reflected electron while $|C_{12}|^2$ gives the probability of a reflected hole in the left TI. Since the current must be the same in all planes we can use this to calculate the conductance in the whole system.

As we have a wave incoming with an amplitude of 1 we can describe the conductance of the system by the formula [12]

$$G = \frac{1}{R_n}(1 - |C_1|^2 + |C_{12}|^2) \quad (15)$$

Here R_n (in Ω) is a constant not dependent on the energy of the particles.

This formula has the interpretation that for a wave function of amplitude 1 describing an electron with a negative charge we get a wave function with amplitude $|C_{12}|^2$ back with a positive charge and $|C_1|^2$ with a negative charge. Thus if we look at the total charge traveling from the left to the right we get $1 - |C_1|^2 + |C_{12}|^2$ which is proportional to the conductance.

In a 2D situation the angle of the particle also plays a role when determining the current. To calculate the current in a system like that the following function can be applied.

$$G = R_n \int_{\pi/2}^{\pi/2} N(\theta)(1 - |C_1(\theta)|^2 + |C_{12}(\theta)|^2)d\theta \quad (16)$$

In formula 16 an integral is taken over θ . This combined with an appropriate weight function $N(\theta)$ will give the current. Since in our system the material in the y-direction always goes from $-\infty$ to ∞ it is appropriate that $N(\theta) = 1$. This is an approximation as for real world cases there will be more particles which travel in a perpendicular direction to the interface in comparison to a parallel direction to the interface.

Since the formulas for C_1 and C_{12} are both complicated the integral mentioned above will not be used. Instead a Riemann sum is used to approximate the integral to save on computing time.

4 Results

As said before the system can be analysed in two different ways. One of the ways is calculating the phase of the system and the other is solving the whole system at once. In section 4.1 the 1D phase equations at each interface are given. In section 4.2 the system is solved for $\theta = 0$ with some results shown in the graphs. The 2D systems are worked out in sections 4.3 and 4.4 for the phase calculations and total system calculations respectively. The last part of the results, section 4.5, gives an overview of the predicted conductance of the system which can be verified using measurements.

4.1 1D phase calculations

In section 3.3.3 and 3.3.2 systems were given with which two of the four reflection constants can be calculated. After doing all calculations the following reflection constants are obtained.

$$\left\{ \begin{array}{l} r_{hh} = \frac{\kappa_h - i(E - M - \mu_m)}{-\kappa_h - i(E - M - \mu_m)} \\ r_{ee} = \frac{-\kappa_e - i(E + M + \mu_m)}{\kappa_e - i(E + M + \mu_m)} \\ r_{eh} = \frac{\Delta}{E + i\sqrt{\Delta^2 - E^2}} \\ r_{he} = \frac{-\Delta}{E + i\sqrt{\Delta^2 - E^2}} \end{array} \right. \quad (17)$$

In the above equation we can see that $r_{eh} = -r_{he}$. This implies that the phase gained by the electron from the reflection at the STI cancels out with the phase the hole gains at the STI. This in turn implies that for an ABS we have $\arg(r_{ee}) + \arg(r_{hh}) = 0$. This only be the case for $E = 0\text{eV}$ so the ABS is always located at $E = 0\text{eV}$ for the 1D situation.

4.2 1D total system

To partly verify the system, the 1D system is analysed. This system should give insight into the function of the different variables of the system which dictate the position of the ABS. Later on this system will be expanded to a 2D system by including the variable for the angle the particle makes with the normal of the interface.

First of, the values for the constants were chosen in such a way that there is a clear Andreev bound state. This implies that $\tilde{M} \gg 0$, $bM \approx 1$, $d\mu < 1$, $\tilde{\mu}_m \approx \tilde{\mu} \approx 0$ and $\tilde{\mu}_S > 0$ if not specified in some other way.

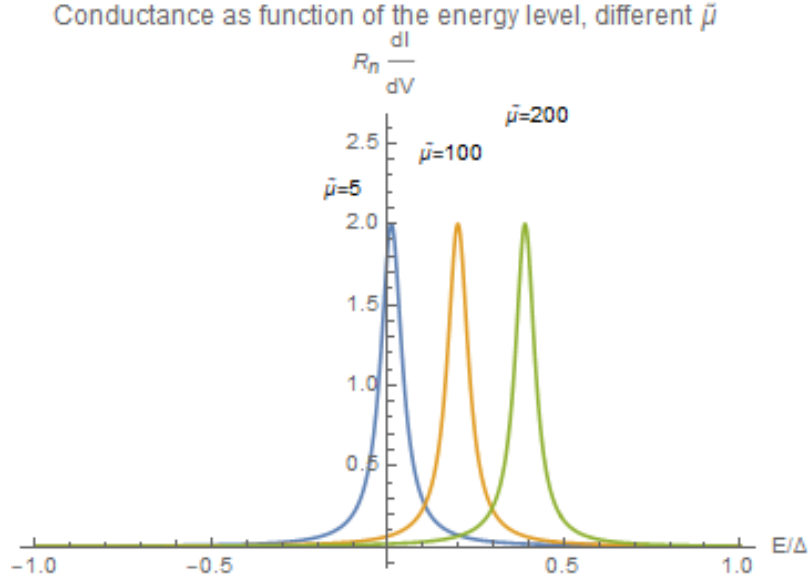


FIGURE 8: In the figure above 3 different value for $\mu_{\tilde{TI}}$ were chosen. We have $d=0.001$.

In figure 8 it can be seen that by changing the chemical potential of the two TIs the peak shifts. This is likely a result of resonance in the TI. The thickness of the TI in this case is 0.001 m. For $\tilde{\mu} = 200$ we can see that $d\mu = 0.2$ which is a significant addition to the phase calculations of an ABS. This implies that the peaks are at different energies because of the phase the wave function gains by traveling through the TI.

4.3 2D phase calculations

In this section and the sections which follow the variables used in calculations will have a set value. These values are $\tilde{M} = 100$, $\tilde{\mu}_S = 100$, $\tilde{\mu}_m = 2$, $\tilde{\mu} = 100$, $d = 0.0005\text{m}$ and $b = 0.01\text{m}$ unless otherwise specified. Also, when a reference is made to $\tilde{\mu}$ this always implies the chemical potential in the TI. In these calculations in this section the thickness of the TI and MTI was not taken into account. Here the ABS are calculated using only the phases the wave function gains at the interfaces.

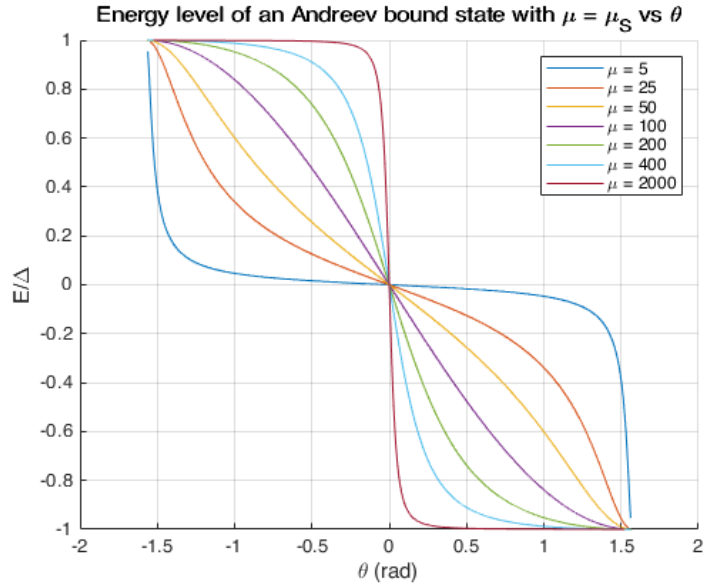


FIGURE 9: In the figure above 7 different value for $\tilde{\mu}$ were chosen. This figure corresponds to the figure represented in [4]. The legend and title are supposed to refer to the dimensionless variables $\tilde{\mu}$ and $\tilde{\mu}_S$.

In figure 9 it can be seen that for a relatively large magnetization M compared to the chemical potential that the ABS stay around 0. However for a large chemical potential the ABS stay around $\theta = 0$.

These can be explained by looking at the formulas for the phase. At the TI/STI, for $\tilde{E} = 0$ interface the phase is $-\pi + 2\theta$ for $\tilde{\mu}_S = \tilde{\mu}$ and for relatively large \tilde{M} at the MTI/TI interface the phase can be approximated by $\pi - 2\theta$ for small θ . This implies that for small theta we and $\tilde{E} = 0$ we have a phase of 0 and thus an ABS.

The latter result can be explained in the same way. For $\tilde{\mu} = \tilde{\mu}_S$ and $\theta = 0$ the phase of the STI cancels as was explained in the 1D calculations. However for a large $\tilde{\mu}$ the phase gained at the MTI is almost 0 for all E thus resulting in an ABS at all energies for $\theta = 0$.

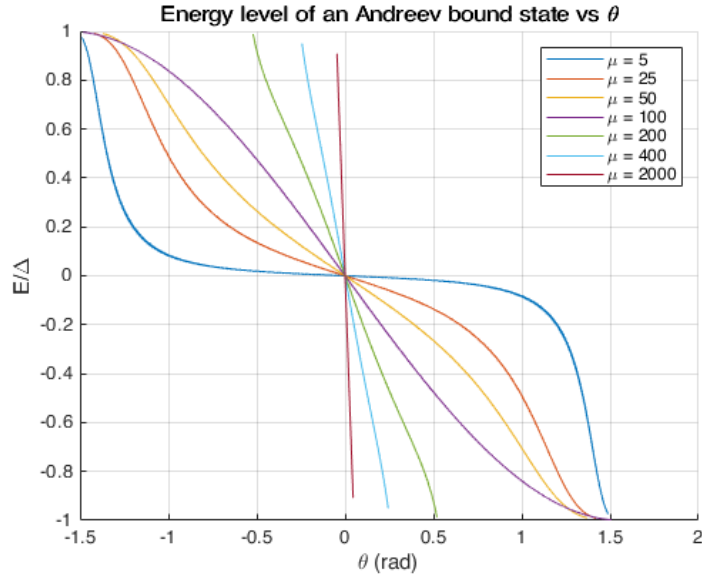


FIGURE 10: Here 7 different values for $\tilde{\mu}$ were chosen and $\tilde{\mu}_S$ was chosen to be 100. The lines which abruptly stop do so because of a numerical issue described in section 3.3.5. The legend and title are supposed to refer to the dimensionless variables $\tilde{\mu}$ and $\tilde{\mu}_S$.

In figure 10 only the $\tilde{\mu}$ was adjusted. This implies that the angles θ is not necessarily equal to θ_S . The consequence of this can easily be spotted for the cases $\tilde{\mu} = 2000$, $\tilde{\mu} = 400$ and $\tilde{\mu} = 200$. In these cases we have that $\frac{\tilde{\mu}_S}{\tilde{\mu}} < 1$ so θ_S is undefined for certain angles. In the other cases where $\frac{\tilde{\mu}_S}{\tilde{\mu}} > 1$ the function behaves just fine.

In the case where $\tilde{\mu}$ is chosen small it seems the function approaches the line $\tilde{E} = 0$. This can be explained by considering that for a small $\tilde{\mu}$ $\theta_S \approx 0$. This results in the same explanation as the figure before. For a small $\tilde{\mu}$ we have a phase added of about $\pi - 2\theta$ and at the STI/TI interface the added phase is close to $-\pi + 2\theta$. Note that I'm considering the total phase at an interface and not just one reflection.

4.4 2D system calculation

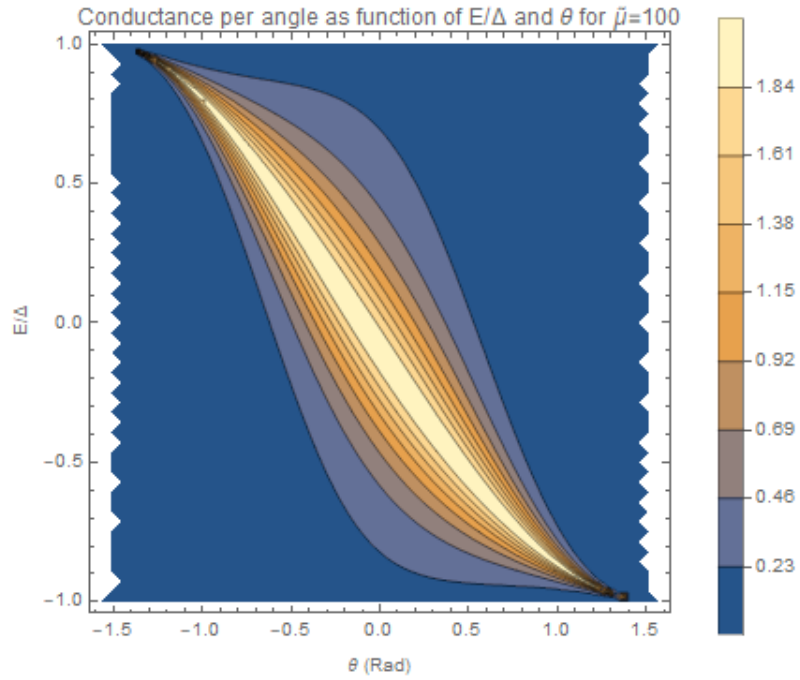


FIGURE 11: This plot has the same values as for plot 9. It only shows the plot for $\tilde{\mu} = 100$. It can be seen that the highest conductance is at the place where the ABS was predicted to be. Conductance per angle is found on the z-axis.

Figure 11 shows a case where the ABS phase calculations and the calculations of the total system coincide. You can see in the contour plot that around the ABS the conductance decreases. This shows the ABS is not a small spike around the ABS but instead a continuous function with a maximum at the ABS.

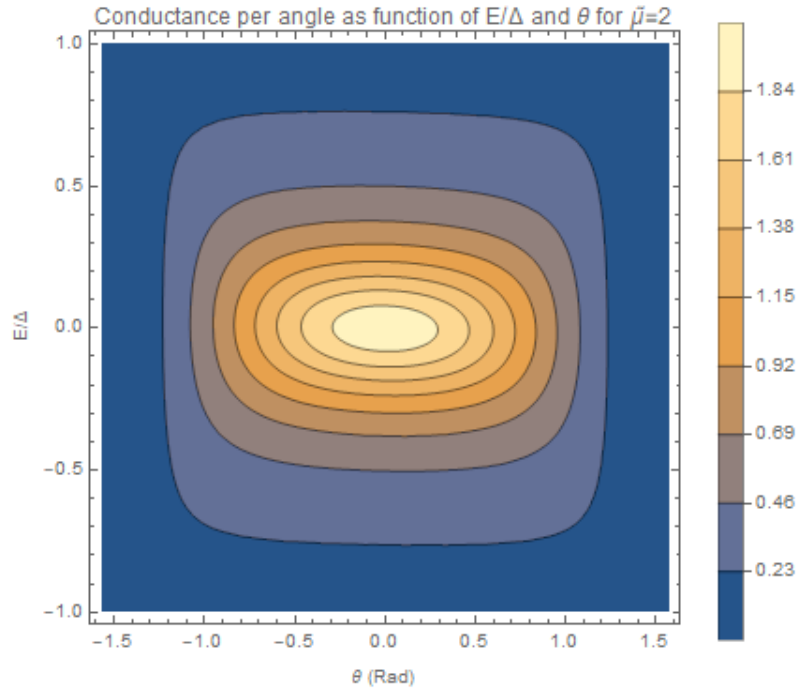


FIGURE 12: In this plot a low $\tilde{\mu}$ was chosen. The plots seems to describe a large ABS in the middle of the plot with a large conductance.

In figure 12 it can be seen that there is an Andreev bound state at $\tilde{E} = 0$. It was predicted by the previous phase calculations that all the ABS should be around $\tilde{E} = 0$ however we can see that while this seems to be the case, at high *theta* the conductance per angle is too low to show this state.

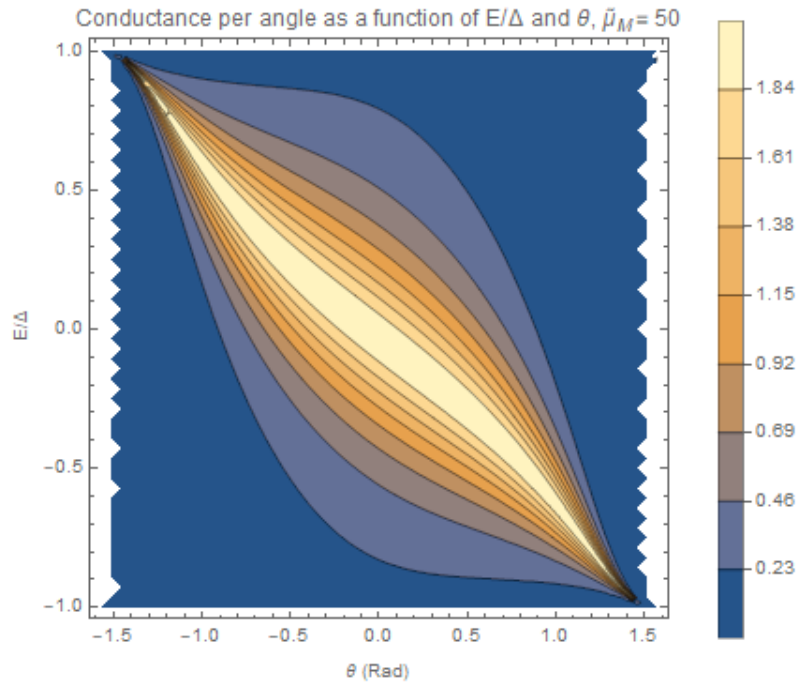


FIGURE 13: In this plot $\tilde{\mu}_M$ was increased. A similar figure can be seen as 11 however this one decreases less around the conductance peaks and curves slightly differently.

When comparing figure 11 and 13 we can see that increasing the chemical potential in the MTI has the effect of pulling the ABS more towards the line $\tilde{E} = 0$. This effect can be seen in its extreme form in the next figure.

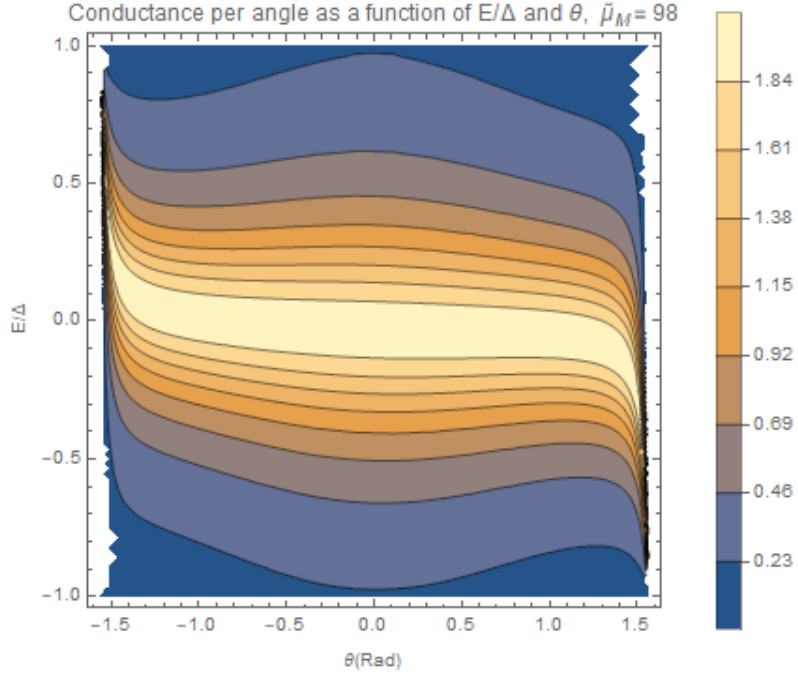


FIGURE 14: Here the same plot was made as in figure 13 however with $\tilde{\mu}_M = 98$. This is thus a more extreme version of the previous plot.

In figure 14 a more extreme plot of figure 13 can be seen. Here it becomes clear that a high $\tilde{\mu}_M$ has the same effect as a low $\tilde{\mu}$. If we plug a high $\tilde{\mu}_M$ in the phase equations for the MTI/TI interface then it is quickly determined that the phase added by this interface is $\pi - 2\theta$ for small θ . Again, around $\tilde{E} = 0$ the phase added by the TI/STI interface is $-\pi + 2\theta$ thus canceling each other.

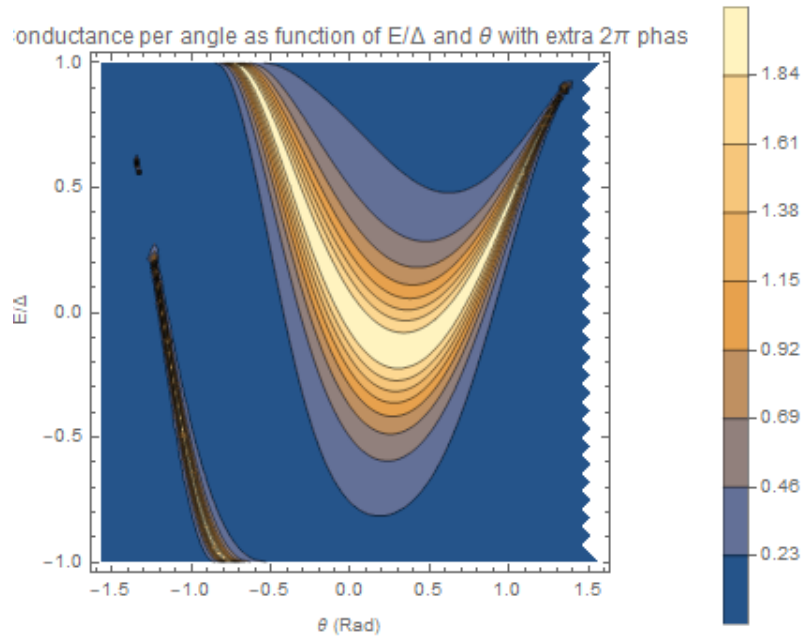


FIGURE 15: In this graph the distance d was chosen such that $d\mu = \pi/2$.

In figure 15 the distance is chosen such that $d\mu = \pi/2$. This should imply that at $\theta = 0$ there is an ABS at $\tilde{E} = 0$. As can be seen in the figure this is indeed the case. Apart from this the figure seems to have shifted. This is expected as an increase in distance not only adds a phase to the ABS at $\theta = 0$ but to all θ . The added phase is however different for all angles which is why the plot does not directly correspond to figure 12.

4.5 System conductance

In the following section a look is taken at the conductance. The conductance as given in equation 16. A Riemann sum is taken with 100 intervals to approximate the conductance itself.

Conductance vs the energy of the particle for $\tilde{\mu} = 2$

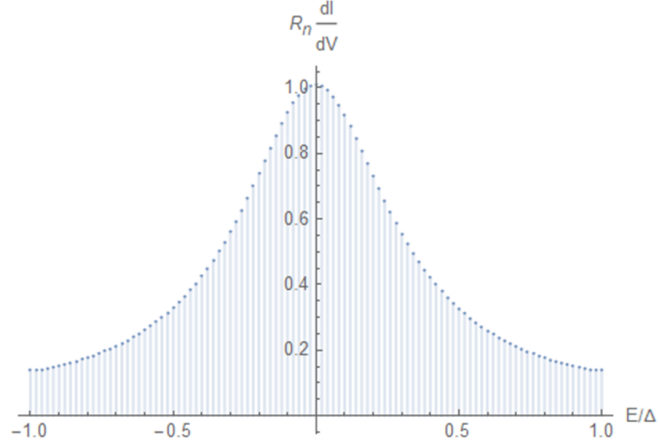


FIGURE 16: Here $\tilde{\mu} = 2$ this implies it resembles the conductance of the figure 12. d is taken small to avoid resonance in the TI.

In figure 16 a clear curve can be seen with a maximum at $\tilde{E} = 0$. This can be explained by considering that at $\tilde{E} = 0$ the largest ABS is located. Around this bound state the transmission of the electron reduces less in comparison to other energies. This gives a peak at $\tilde{E} = 0$ which decreases with different energies.

Conductance vs the energy of the particle for $\tilde{\mu} = \tilde{\mu}_s = 20$

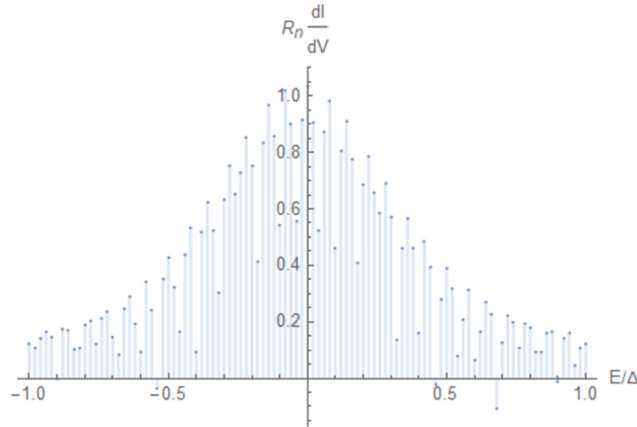


FIGURE 17: In this graph we have $\tilde{\mu}_s = \tilde{\mu} = 20$ which is considerable lower than the magnetization M which is 100. d is taken small to avoid resonance in the TI.

In figure 17 you can see a similar curve compared to figure 16. The curve is however not as smooth, as the ABS are located in very specific points along the θ -axis and decrease rapidly around that. It is also clear that there is a maximum at $\tilde{E} = 0$ because of many bound states close to $\tilde{E} = 0$ as could be concluded from figure 9.

Conductance vs the energy of the particle for $\tilde{\mu}_m = 98$ and $\tilde{\mu} = 100$

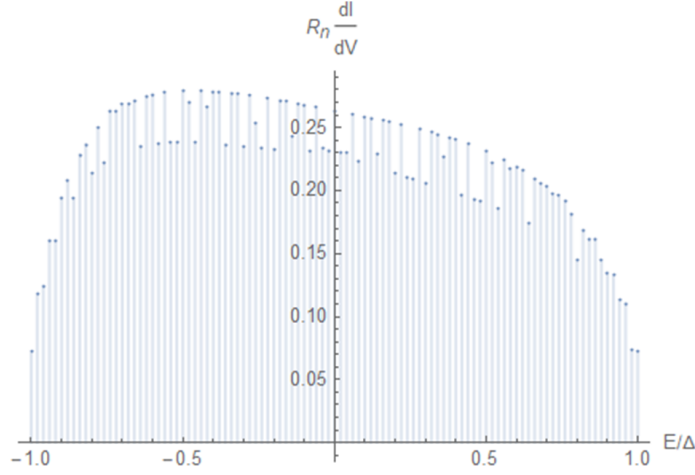


FIGURE 18: In this graph we have $\tilde{\mu} = \tilde{\mu}_S = M = 100$. Apart from this the distance d is taken small.

In figure 18 the conductance is given. The conductance is relatively high for a large number of energies. This is the result of the ABS which is present in equal amounts along the whole graph for $\tilde{\mu} = 100$, just like in 9 and 11.

Conductance vs the energy of the particle for an extra phaseshift of 2π

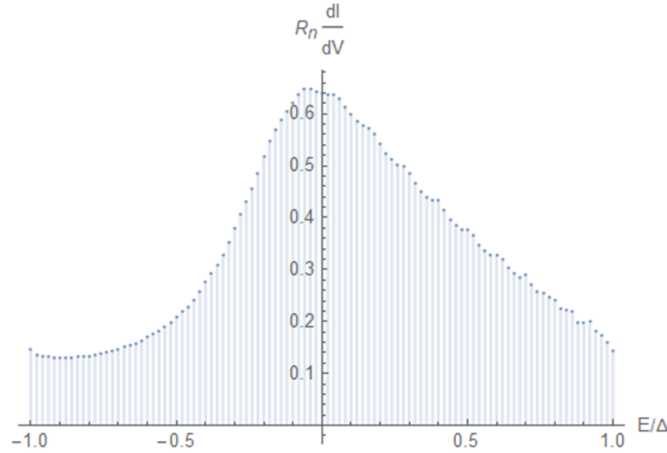


FIGURE 19: In this graph the conductance as a function of the energy is shown. The calculations were done for $d\mu = \pi/2$ and $\tilde{\mu}_S = \tilde{\mu} = \tilde{M} = 100$.

In figure 19 a graph is plotted of the theoretical conductance for $d\mu = \pi/2$. The result shows an asymmetric conductance instead of a symmetric one shown in the previous conductance graphs. This asymmetry is a direct result of the added phase by the TI. As the shift was exactly 2π for $\tilde{E} = 0$ the peak is still expected to be at $\tilde{E} = 0$. However at different energies an asymmetry is expected as there is no clear symmetry in the added phases by the reflection constants which does not rely on an added phase in the TI.

5 Discussion

In this section a few points will be addressed. Firstly, a look will be taken at the calculations to see what is mathematically and physically not represented. Then suggestions will be made for further expansion of the model.

5.1 Limitations of the model

Throughout the thesis multiple restrictions have already been given which influence what can be checked with this model and what can't. The restrictions which were noticed early on are that $M > \mu_m > 0$, $\mu_S, \mu > 0$, $\Delta \geq |E|$. These all have to do with the spinors which were determined in the theory section. If values which differ from these values are chosen there is little certainty that the theory is accurate.

However that is not the only limitation of the model. To arrive at the equations in the theory θ_S was approximated to be $\theta_S = \arctan(\frac{k_y}{k_x})$ however in the STI there is also an evanescent wave present. This causes the previous equation not to be true for all θ but instead approximates it. The degree in which this approximation is correct was not investigated.

During the derivation of the spinors of the STI the assumption was made that if the spinor was solved for $E > 0$ this would also apply to $E < 0$. This assumption should be checked for future work with this basis. Also, when the spinors were determined the Andreev Approximation was used which can be made if $\Delta, E \ll \epsilon_f$. While this assumption is true for the model, it is an approximation nonetheless.

Later on it was noticed that while Mathematica can calculate specific functions easily, when using large functions this takes a lot of time, especially regarding contour plots. In these contour plots around the lines $\theta = \pi/2$ and $\theta = -\pi/2$ some anomalies can be seen in multiple plots. These exist as instabilities in the plotting algorithm for Mathematica and do not have real values as expected however on the lines themselves this is not necessarily the case.

5.2 Expansion of the model

There are ample ways to expand this model into something that reflects reality better. One major improvement is the calculation of the conductance in a 2D situation. In this thesis a Riemann sum was used to approximate the integral, however if this integral could be directly calculated or a more accurate Riemann sum could be taken this would already improve the result.

Also, in the calculations of the conductance $N(\theta)$ was taken to be 1 for all θ . In reality this is not accurate as a weighed function with weights such that $N(\theta)$ attains its maximum at $\theta = 0$ and its minimum for $\theta = \pi/2$ or $\theta = -\pi/2$.

6 Conclusion

By using the theory now established for Topological insulators it is possible to create a complex model in which the conductance in a 2D situation can be calculated. While the exact results still need to be empirically verified this system is a promising case in which ABS can be used to get a specific conductance at a certain voltage. The locations of the

ABS can be easily predicted by a phase calculation however to get the actual conductance all variables need to be calculated in the whole system.

7 Future experiments

As was said before the results of this thesis will need to be verified. This can be done by constructing a setup using the different TIs described in this thesis and measuring the conductance of this system. If this proves to be correct the model could be developed further with even more generalizations.

Nomenclature

α	Phase of the reflection
\mathbf{q}	A phonon
Δ	Superconducting Gap
ϵ_f	Fermi energy
\hbar	Planck constant
μ	Chemical potential of the TI
μ_m	Chemical potential of the MTI
μ_S	Chemical potential of the STI
ω_D	Debye frequency
Ψ	Basis of the system
ψ	Spinor in the system
θ	Angle the particle makes compared to the normal vector of the interface
θ_S	The angle of the particle in the STI compared to the normal to the interface
\tilde{E}	Energy normalised, for others see section 3.1
E	Energy of the particle compared to the fermi energy
H	Hamiltonian of the material
k_x	Wave vector in the x-direction
k_y	Wave vector in the y-direction
M	Magnetization of the MTI
R_n	Normal resistance
u_k, u	Squareroot of the change of a hole occupying the referred to state
v_k, v	Squareroot of the change of a hole occupying the referred to state
ABS	Andreev bound state
b	Width of the MTI
d	Width of the middle TI
MTI	Magnetic topological insulator

STI Superconducting topological insulator

TI Topological Insulator

References

- [1] Yoichi Ando. Topological insulator materials. *Journal of the Physical Society of Japan*, 82(10):102001, 2013.
- [2] Frank Wilczek. Majorana returns. *Nature Physics*, 5(9):614–618, Sep 2009.
- [3] V. Mourik, K. Zuo, S. M. Frolov, S. R. Plissard, E. P. A. M. Bakkers, and L. P. Kouwenhoven. Signatures of majorana fermions in hybrid superconductor-semiconductor nanowire devices. *Science*, 336(6084):1003–1007, Apr 2012.
- [4] Yukio Tanaka, Takehito Yokoyama, and Naoto Nagaosa. Manipulation of the majorana fermion, andreev reflection, and josephson current on topological insulators. *Phys. Rev. Lett.*, 103:107002, Sep 2009.
- [5] J. Bardeen, L. N. Cooper, and J. R. Schrieffer. Theory of superconductivity. *Phys. Rev.*, 108:1175–1204, Dec 1957.
- [6] V.V. Schmidt. *The Physics of Superconductors*. Springer, 1997.
- [7] Crimson Academies Dux College. Cooper-pair-phonon, 2020. Last accessed 15 June 2020.
- [8] Cui-Zu Chang, Jinsong Zhang, Xiao Feng, Jie Shen, Zuocheng Zhang, Minghua Guo, Kang Li, Yunbo Ou, Pang Wei, Li-Li Wang, Zhong-Qing Ji, Yang Feng, Shuaihua Ji, Xi Chen, Jinfeng Jia, Xi Dai, Zhong Fang, Shou-Cheng Zhang, Ke He, Yayu Wang, Li Lu, Xu-Cun Ma, and Qi-Kun Xue. Experimental observation of the quantum anomalous hall effect in a magnetic topological insulator. *Science*, 340(6129):167–170, 2013.
- [9] A. Brinkman. Private notes, 2020.
- [10] Chuan Li, Jorrit C. de Boer, Bob de Ronde, Shyama V. Ramankutty, Erik van Heumen, Yingkai Huang, Anne de Visser, Alexander A. Golubov, Mark S. Golden, and Alexander Brinkman. periodic andreev bound states in a dirac semimetal. *Nature Materials*, 17(10):875–880, Oct 2018.
- [11] Wikipedia. Andreev reflection, 2020. Last accessed 15 June 2020.
- [12] G. E. Blonder, M. Tinkham, and T. M. Klapwijk. Transition from metallic to tunneling regimes in superconducting microconstrictions: Excess current, charge imbalance, and supercurrent conversion. *Phys. Rev. B*, 25:4515–4532, Apr 1982.